



# Integrative epigenomic profiling reveal AP-1 is a key regulator in intrahepatic cholangiocarcinoma

Ke He<sup>a,b</sup>, Yuliang Feng<sup>c</sup>, Sanqi An<sup>a,b</sup>, Fei Liu<sup>a</sup>, Guoan Xiang<sup>a,\*</sup>

<sup>a</sup> Department of General Surgery, Guangdong Second Provincial General Hospital, Guangzhou 510317, China

<sup>b</sup> Department of Biochemistry, Zhongshan School of Medicine; Center for Stem Cell Biology and Tissue Engineering, Key laboratory of ministry of education, Sun Yat-sen University, Guangzhou 510080, China

<sup>c</sup> Botnar Research Centre, Nuffield Department of Orthopaedics, Rheumatology and Musculoskeletal Sciences, University of Oxford, OX37LD, United Kingdom

## ARTICLE INFO

### Keywords:

Intrahepatic cholangiocarcinoma  
Histone modification  
Nucleosome positioning  
Data analysis  
AP-1

## ABSTRACT

Intrahepatic cholangiocarcinoma (ICC) is a malignant tumor with poor prognosis while its mechanisms of pathogenesis remain elusive. In this study, we performed systemic epigenomic and transcriptomic profiling via MNase-seq, ChIP-seq and RNA-seq in normal cholangiocyte and ICC cell lines. We showed that active histone modifications (H3K4me3, H3K4me1 and H3K27ac) were less enriched on cancer-related genes in ICC cell lines compared to control. The region of different histone modification patterns is enrichment in sites of AP-1 motif. Subsequent analysis showed that ICC had different nucleosome occupancy in differentially expressed genes compared to a normal cell line. Furthermore, we found that AP-1 plays a key role in ICC and regulates ICC-related genes through its AP-1 binding site. This study is the first report showing the global features of histone modification, transcript, and nucleosome profiles in ICC; we also show that the transcription factor AP-1 might be a key target gene in ICC.

## 1. Introduction

Intrahepatic cholangiocarcinoma (ICC) is the second most common primary hepatic malignancy. It has a poor prognosis with a 5-year survival of less than 20% [1]. In addition, the number of new cases of ICC is increasing, and the ICC-related mortality rate increased from 2.9 to 5.0 per 100,000 males and from 2.7 to 4.6 per 100,000 females in recent years [1]. The pathogenesis of ICC remains unclear and there are currently no effective treatments, representing the two greatest challenges associated with this disease [2]. Thus, a better understanding of the molecular mechanisms underlying ICC is needed.

Epigenetic modification, including H3K4me1 and nucleosome occupancy, is involved in cancer genesis through essential cancer-related genes [3,4,5,6,7,8,9,10,11]. For example, previous studies reported that H3K4me3 might be increased in breast, kidney, and colon cancers and correlated with a poor clinical outcome [12]. H3K4me3 is also associated with tumor progression and favorable prognosis in colorectal cancer [5]. H3K4me1-marked genes promote colon carcinogenesis, while many cancer-associated genes exhibit H3K27ac modification [13]. The cross-talk between nucleosome and histone modification affect tumor biology. For instance, nucleosome occupancy is a great marker for

early estimation of the response to therapy in colorectal cancer patients [14]. Nucleosome positioning influences breast cancer metastasis through splice site recognition [15]. However, there is limited research on whether epigenetic modification and nucleosome occupancy are associated with ICC. Previous studies prefer to focus on the role of non-coding RNA (ncRNA), DNA methylation, histone methylation enzyme rather than real dynamic histone modifications levels and nucleosome localization [16,17].

Recent research reports that c-JUN/AP-1 involvement in chromatin remodeling plays an important role in epigenetic control of transcription [18], and could regulate cancer-related genes involved in the metastasis of cancer [19,20], although there have not been any studies published on the role of AP-1 in ICC. Given that both nucleosome density and histone modifications affect cancer-related gene expression, we analyzed ChIP-seq, RNA-seq, and MNase-seq datasets from the four most widely used intrahepatic cholangiocarcinoma cell lines (SSP-25, HUCCT1, CCLP-1, and TFK-1) and a human intrahepatic biliary epithelial cell line (HIBEpiC) to determine whether ICC is associated with histone modification and nucleosome positioning [21,22,23,24,25]. Integrated analysis of nucleosome accessibility with histone modification states in ICC has improved our understanding of

\* Corresponding author at: 466 Xingangdong Road, Guangzhou 510317, China.  
E-mail address: [guoan\\_66@163.com](mailto:guoan_66@163.com) (G. Xiang).

<https://doi.org/10.1016/j.ygeno.2021.12.008>

Received 22 August 2020; Received in revised form 19 April 2021; Accepted 14 December 2021

Available online 20 December 2021

0888-7543/© 2021 The Authors.

Published by Elsevier Inc.

This is an open access article under the CC BY-NC-ND license

(<http://creativecommons.org/licenses/by-nc-nd/4.0/>).

epigenetic modifications and nucleosome profiles in ICC. Our results revealed the molecular mechanism of ICC and indicated that AP-1 may be a therapeutic target of ICC.

## 2. Materials and methods

### 2.1. Cell culture and antibodies

SSP-25, CCLP-1, TFK-1, HuCCT1, and HIBepic cells were purchased from Guangzhou Jennio-bio (Guangzhou Jennio-bio Co., Ltd., Guangzhou, China). All cells were maintained in Roswell Park Memorial Institute 1640 medium (Gibco, Invitrogen, Carlsbad, CA, USA) supplemented with 10% fetal bovine serum (FBS; Gibco/BRL, MD, USA), 100 U/mL penicillin, and 100 mg/mL streptomycin (Beyotime Biotechnology Co., Ltd., Shanghai, China). The cells were cultured at 37 °C in 5% CO<sub>2</sub>. All experiments were performed with mycoplasma-free cells. Antibodies against c-JUN (66313–1-Ig), and c-FOS(66590–1-Ig) were purchased from Proteintech Group (Rosemont, IL, USA); antibodies against GAPDH (sc-47,724) were purchased from Santa Cruz Biotechnology, Inc. (Santa Cruz, CA, USA).

### 2.2. Transient transfection and establishment of stably expressing cells

A small interfering RNA (siRNA) targeting the c-FOS transcript and a nonspecific control siRNA were purchased from GeneCreate Biological (Wuhan GeneCreate Biological Engineering Co., Ltd., Wuhan, China). The target sequences for the c-FOS transcript were as follows: siRNA-1: GGAACAGUUAUCUCCAGAATT; siRNA-2: UCUCAGUGCCAACUUCAUUTT; siRNA-3: GACAGACCAACUAGAAGAUUTT; and siRNA-4: CCAACUAGAAGAUGAGAAGTT. The specific siRNA or negative control was transfected into ICC cells with Lipofectamine 2000 transfection reagent (Invitrogen) according to the manufacturer's instructions. For establishment of stable c-JUN overexpressing cells, an overexpression plasmid was constructed and packed with a lentivirus system by GeneCreate Biological. After removing the medium, lentiviral supernatant was added (with 6 µg/mL polybrene). After 24 h, the supernatant was removed and cells were selected for 4 weeks using DMEM with 10 µg/mL puromycin (Sigma-Aldrich, St. Louis, MO, USA).

### 2.3. RNA-seq

Total RNA was extracted from SSP-25, CCLP-1, TFK-1, HuCCT1, and HIBepic cells using TRIzol reagent (Invitrogen) according to the manufacturer's instructions. RNA quality was evaluated with a BioAnalyzer 2100 system (Agilent Technologies, Santa Clara, CA, USA). Small RNAs had linkers ligated to them and bar-coded cDNAs were prepared using a TruSeq Sample Prep Kit (Illumina, San Diego, CA, USA) according to the manufacturer's instructions. Individual libraries were analyzed for the presence of linked cDNA at the appropriate size (140–150 bp) as determined by the BioAnalyzer. Subsequently, the amplified cDNA constructs were agarose gel-purified in preparation for sequencing analysis using the Illumina HiSeq 2500 platform (Illumina) according to the manufacturer's instructions at the Shanghai Biotechnology Corporation.

The RNA sequence reads were pre-processed using the FASTXToolkit to exclude low-quality reads (ambiguous N, quality <10 nt, and length < 18 nt) and 3' adapter, 5' adapter, and poly(A) sequences. Further annotation analyses were performed using the commercial software CLC Genomic Workbench 5.5. After all the annotation steps, the sequencing libraries were used for size distribution and saturation analysis.

### 2.4. ChIP and ChIP-seq

ChIP experiments were performed as previously described using the anti-H3K4me1 antibody (ab8895; Abcam, Cambridge, UK), anti-H3K4me3 antibody (ab8580; Abcam), anti-H3K27ac antibody

(ab4729; Abcam) and anti-c-JUN antibody (ab32137; Abcam). The cells were crosslinked with formaldehyde treatment and chromatin was fragmented to 200–300 bp by sonication. Chromatin from 10<sup>7</sup> cells was used for each ChIP experiment, which yielded approximately 200 ng of DNA. Protein A dynabeads (product no. 100.02) were added to chromatin extracts for 2 h at room temperature with rotation. The beads were washed twice with 1 × phosphate-buffered saline (PBS) and 1 × PBS and 2 µg antibody was added to the beads. The samples were incubated for 2 h on the mixer at 4 °C to allow complete antibody binding to the beads. The beads were washed five times and resuspended in 1 × TE. Then, 10% SDS and 20 mg/mL proteinase K were added and the samples were incubated at 65 °C overnight. ChIP DNA was extracted using phenol/chloroform. ChIP DNA library construction was conducted with the NEBNext Ultra DNA Library kit according to the manufacturer's instructions (E7370; NEB, Ipswich, MA, USA) [26].

### 2.5. MNase-seq

The cells were trypsinized and pelleted prior to washing and resuspension in digestion buffer (50 mM Tris-HCl, pH 7.6, 1 mM CaCl<sub>2</sub>, and 0.2% Triton X-100 or NP-40). Then, 5 mM butyrate, 1 × proteinase inhibitor cocktail, and fresh 0.5 mM PMSF was added and cells were digested with MNase (Sigma-Aldrich) for 5 min at 37 °C. The reactions were terminated by the addition of an equal volume of stop buffer (10 mM Tris, pH 7.6, and 5 mM EDTA) and sonicated for 5 min in the cold room in ice water. DNA was extracted using phenol/chloroform. The isolated DNA was run out on a gel, and DNA fragments approximately 200 bp long were gel-selected. The libraries were prepared according to the Illumina library preparation protocol. MNase-seq libraries were sequenced at the Beijing Genomic Institute.

### 2.6. Apoptosis analysis

Apoptotic cells were stained with Annexin V/PI Staining Kit (KeyGEN BioTECH, Shanghai, China) and detected by CytoFLEX (Beckman Coulter). The experiments were performed in triplicate. The results represent the means ± standard deviation. FlowJo7.6.1 software was used to analyze the ratio of apoptotic cells.

### 2.7. Western blotting

Proteins from ICC cell extracts were separated by SDS polyacrylamide gel electrophoresis. Proteins were transferred onto a polyvinylidene fluoride membrane and incubated for 60 min in 0.05% Tween-20 in phosphate-buffered saline with 5% dried skim milk at room temperature. Immunoblot analysis was performed using the appropriate primary antibody at 4 °C for 12 h. After three washes, the membranes were incubated with a horseradish peroxidase-conjugated secondary antibody for 60 min. Immunoreactive bands were visualized with an enhanced chemiluminescent detection kit (Beyotime Biotechnology Co., Ltd.).

### 2.8. Quantitative real-time PCR

Total RNA was isolated from cell lines using an RNA isolation kit (Takara Biomedical Technology (Beijing) Co., Ltd.). We used MMLV reverse transcriptase to synthesize cDNA. A SYBR Green reaction system (Takara Biomedical Technology (Beijing) Co., Ltd.) was used to amplify the cDNA. The differences in c-JUN, c-FOS, and CCND2 mRNA expression were normalized to GAPDH RNA levels. Primers we designed are shown in Supplementary Table S1.

### 2.9. Data analysis

RNA-seq data was mapped to hg19 using hisat2 and cufflinks were used to calculate the gene expression level in all samples [27,28].

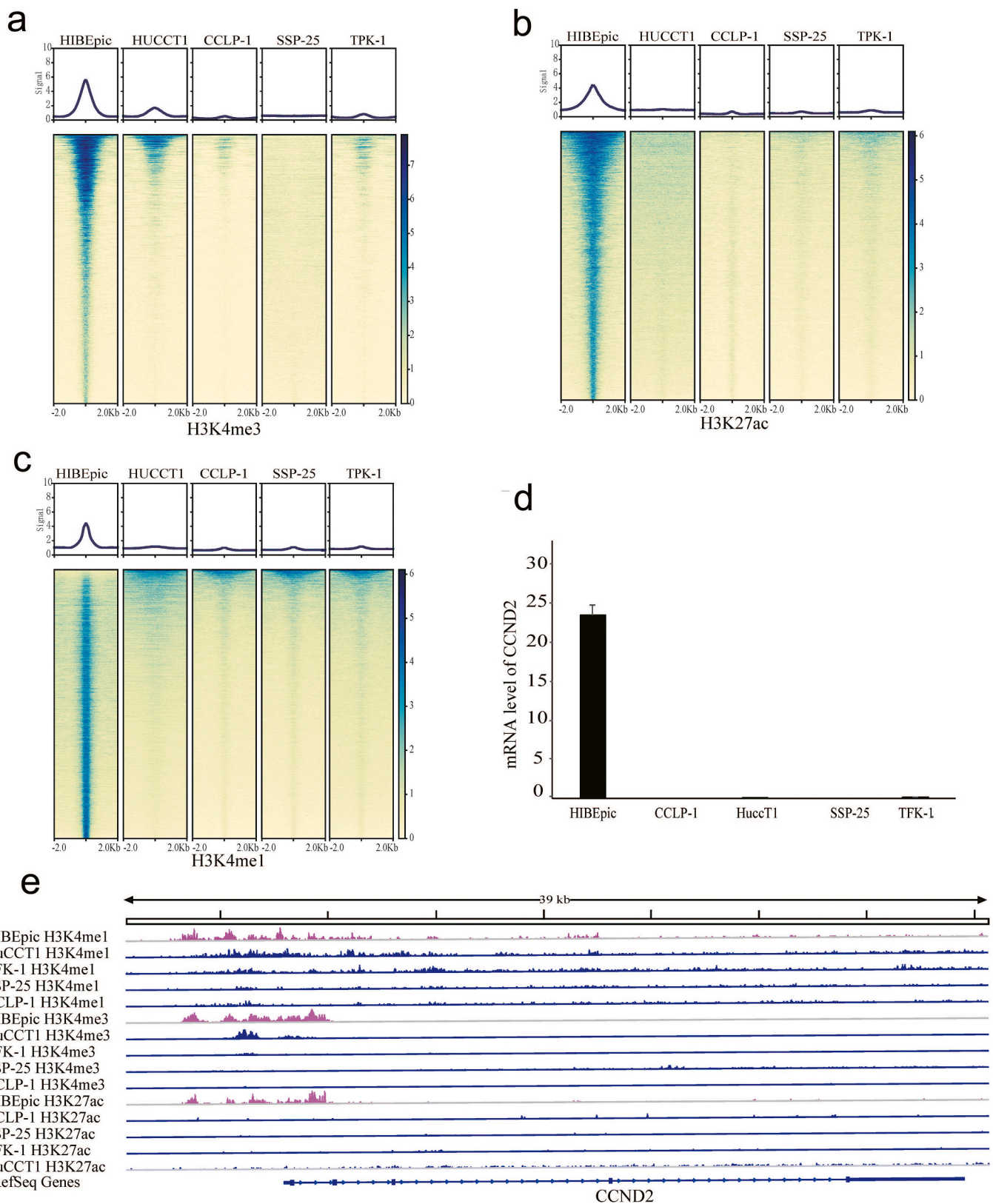


**Fig. 1.** Different ChIP-seq profiles between normal and cancer cell lines, illustrating an example of lost variant promoter loci and variant enhancer loci. Heatmaps show the corresponding ChIP-seq signals  $\pm 2$  kb of variant promoter loci and variant enhancer loci midpoints. **d.** Bar plot representing CCND2 expression in these samples. **e.** H3K4me3, H3K4me1, and H3K27ac ChIP-seq signals across the CCND2 locus, associated with a lost variant promoter loci and variant enhancer loci in these samples.

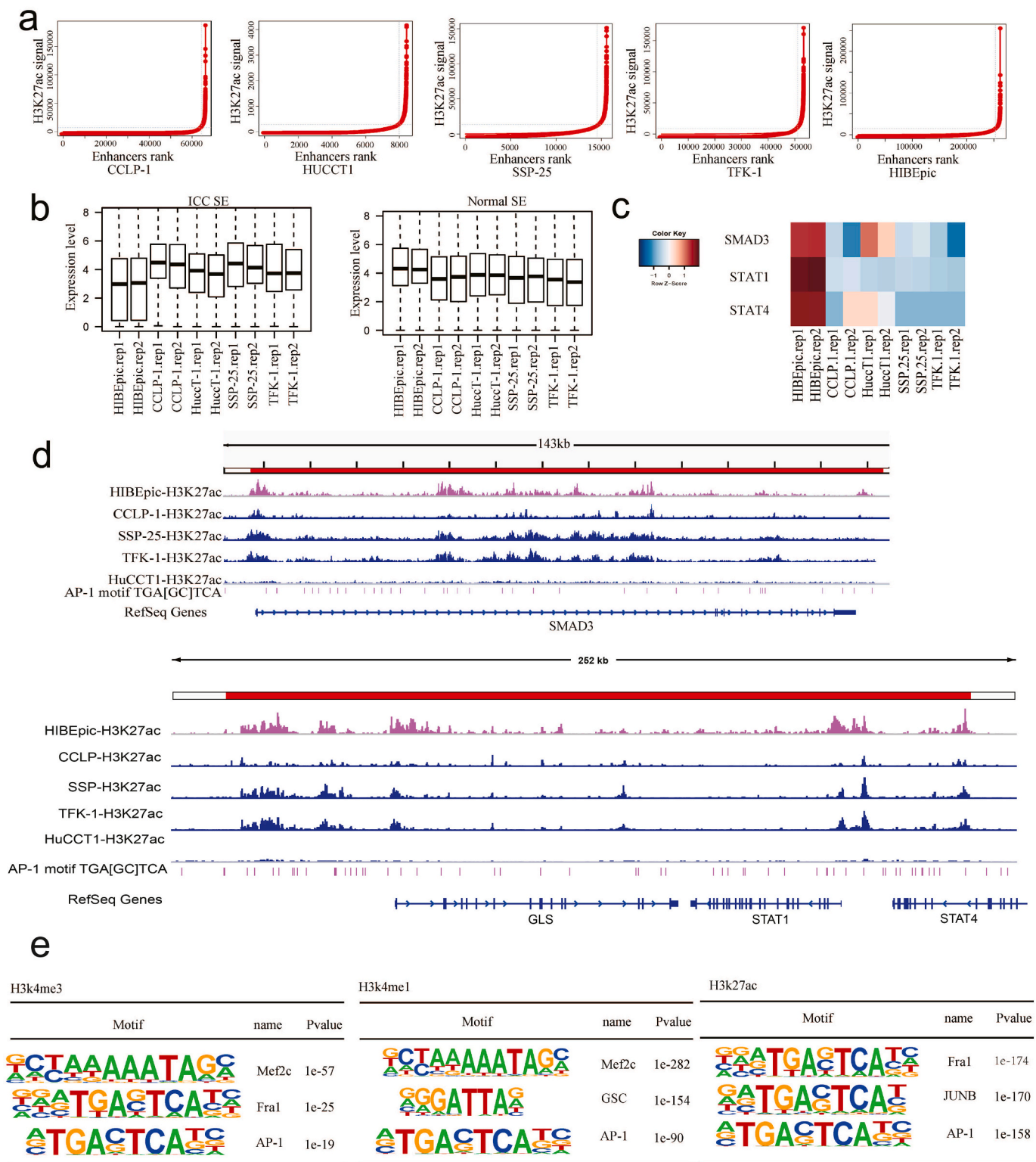


**Fig. 2.** Associates with lineage-specific super enhancers (SEs). **a.** Identification of human ICC cancer cell line SE by H3K27ac ChIP-seq signal. **b.** Transcriptome profiling of the cell lines shows significantly higher gene expression in SEs. **c.** H3K27ac ChIP-seq signals across the SMAD3 and STAT1 loci, associated with lost variant enhancer loci in these samples. **d.** Heatmap representing the expression levels of SMAD3, STAT1, and STAT4 in the cell lines. **e.** Motif enrichment analysis at variant promoter loci and variant enhancer loci.

Quantile normalizations of the gene expression level were performed.  $FDR < 0.1$  and  $|\log_2(\text{fold change})| > 1$  were set as the cutoff for DEGs. A total of 2195 DEGs were identified between the cancer cell lines and the normal cell line.

We used the MACS2 call peak tool to identify peaks along the

genome, HOMER software was used for motif enrichment analysis [29]. We analyzed the MNase-seq data with Bowtie2 and Danpos tools [30,31]. Then, R software and the bioconductor package “diffbind” and a one sample *t*-test were used to calculate the variance of epigenetic modifications in different samples [32]. To view peak details, IGV

software was used to view the specific track [33]. The raw sequence reads have been deposited at <https://www.ncbi.nlm.nih.gov/sra> (accession nos. PRJNA588522 and SUB6386682 Reviewer link: <https://dataview.ncbi.nlm.nih.gov/object/PRJNA588522?reviewer=j5aahcvj3aj9qmlbg9q649g2e7>). ICC patients with liver cancer in the The Cancer Genome Atlas (TCGA) were used as the validation data. Gene function annotations were performed using the DAVID database [34], and GeneMANIA software and TCPA databases were also used as validation data. Kaplan–Meier survival analysis was performed to examine the survival of patients. A two-tailed Student's *t*-test was used to analyze differences between two groups. *P*-values were provided for each comparison. Blind analysis was not involved in this study.

## 2.10. Tissue specimens

This research was conducted under the approval and supervision of the Ethics Committee of Guangdong Second Provincial General Hospital. 41 ICC patients without any preoperative chemotherapy or radiation therapy had signed the written informed consent before study. The cancer and paracancerous tissues were obtained after surgery, and each patient's cancer was confirmed by pathological diagnosis as intrahepatic cholangiocarcinoma. ICC tissues were instantly stored at  $-80^{\circ}\text{C}$  in liquid nitrogen till RNA extraction. All cancer and paracancerous were subjected to qPCR to detect *c-JUN*, *c-FOS*, and *CCND2* mRNA expression levels, and were divided into high and low groups according to the median qPCR relative expression value of cancer tissues. Kaplan–Meier survival analysis was performed to examine the survival of patients.

## 2.11. Immunohistochemical staining

The cancer and paracancerous tissues from all cases were diagnosed by two certificated pathologists without discrepancy. The paraffin-embedded tissues were first stained with hematoxylin and eosin (HE) for histological examination. Subsequently, deparaffinized sections were treated with 3%  $\text{H}_2\text{O}_2$  and subjected to antigen retrieval by citric acid (pH 6.0). After overnight incubation with primary antibody (anti-*c-JUN* antibody; Abcam, Cambridge, UK) by 1:200 at  $4^{\circ}\text{C}$ , sections were incubated for 15 min at room temperature with horseradish peroxidase-labeled polymer conjugated secondary antibody (MaxVision Kits) and incubated for 1 min with diaminobenzidine. The sections were then lightly counterstained with hematoxylin. The sections without primary antibody served as negative controls. Expression level of *c-JUN* was determined according to the average score of two pathologists' evaluations.

## 3. Results and discussion

### 3.1. ICC cell lines have increased histone modification compared with a normal cell line

SSP-25, HUCCT1, CCLP-1, and TFK-1 are the most common cancer cell lines used in ICC. Human Intrahepatic Biliary Epithelial Cells (HIBEpiC) is normal cholangiocyte cell line. To obtain epigenetic modification profiles in ICC cell lines and the normal cell line, we performed ChIP sequencing (ChIP-seq) in these cell lines. Interestingly, the results showed different modification profiles between the ICC cell lines and the normal cell line using the “diffbind” package (Supplementary Fig. S1). H3K4me1, H3K4me3, and H3K27ac marks were low-enriched in ICC cell lines, compared with the normal cell line (Fig. 1a–c). The GO enrichment analysis of the differently enriched H3K4me1, H3K4me3, and H3K27ac sites in ICC indicated that GO function for three histone modifications types are nephron tubule epithelial cell differentiation, glomerular filtration, and cell differentiation (Fig. S1). These differently enriched histone modifications targets a number of genes including *CCND2*. The cell cycle-related gene *CCND2* has been shown to be important in phosphorylation of the tumor suppressor protein Rb.

Previous studies have suggested this gene plays an essential role in many types of cancers [35,36,37,38]. High expression of this gene was observed in ovarian tumors [39]. It has also been reported that *CCND2* may play a key role in cholangiocarcinoma and could be regulated by transcription factors (e.g., TCF/LEF family members) [39]. Expression level of *CCND2* was lower in the cancer cell lines than the normal cell line (Fig. 1d). As showed in ChIP-seq, *CCND2* had higher H3K4me1, H3K4me3, and H3K27ac signal compared with the normal cell line (Fig. 1e).

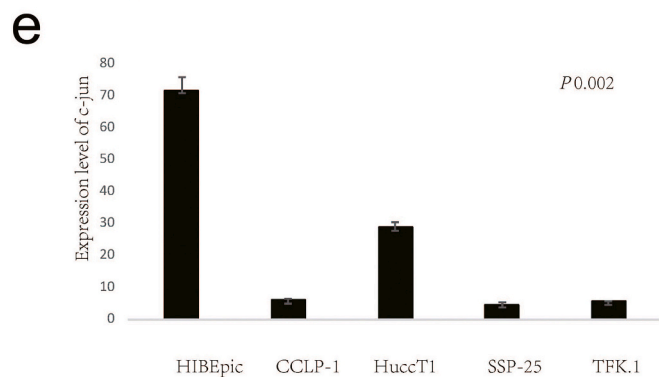
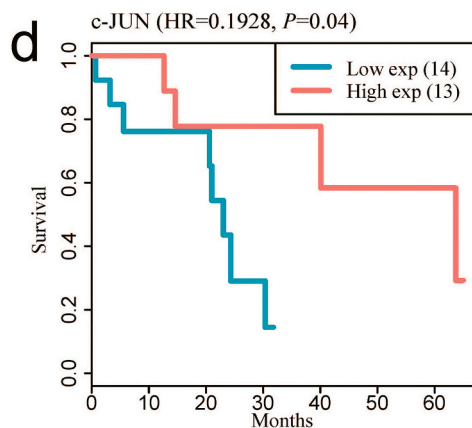
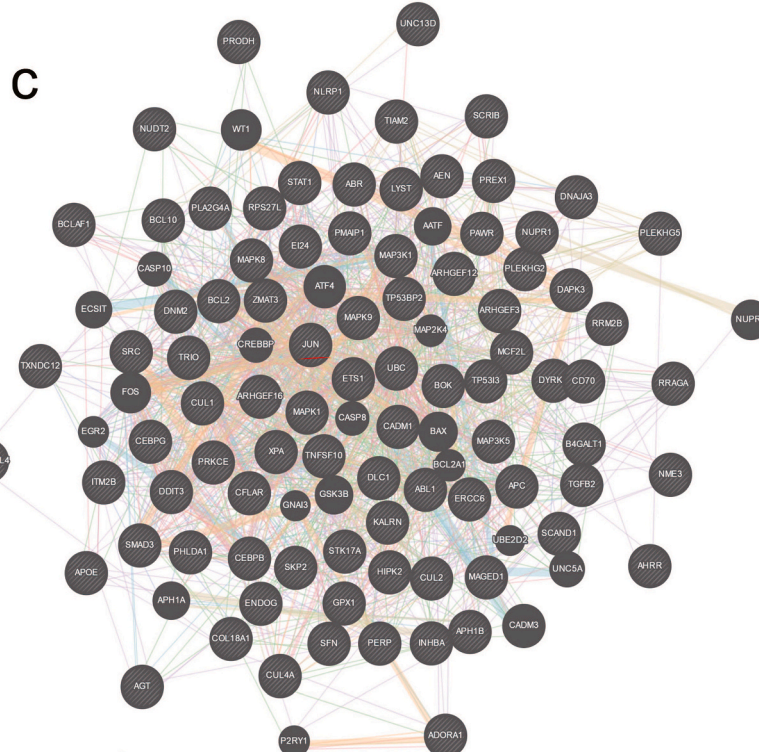
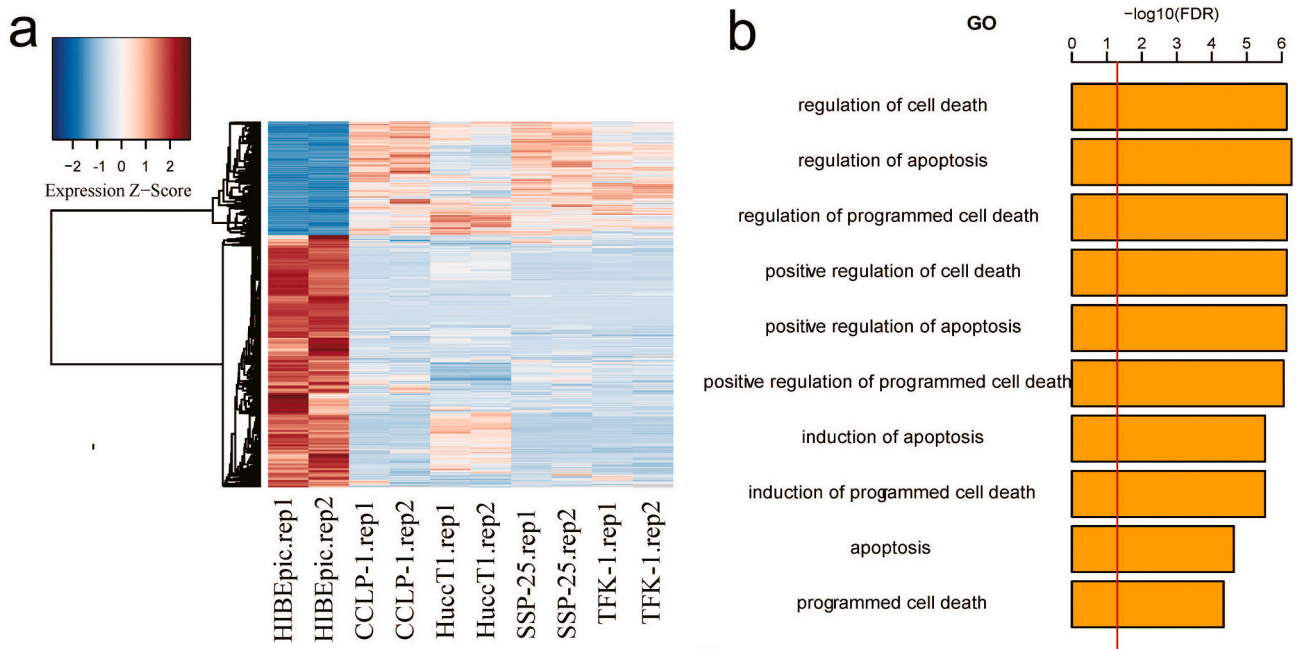
### 3.2. ICC-specific super enhancers affect gene expression in ICC and the region of different histone modification patterns are enrichment in sites of AP-1 motif

As shown in Fig. 2, we first identify Super-Enhancers (SEs) using H3K27ac in the genomes of HIBEpiC, SSP-25, HUCCT1, CCLP-1, and TFK-1 cells, H3K27ac is an indicator of active enhancers. The algorithm ROSE was used to stitch peaks within 12.5 kb and ranked them by signal intensity [40]. We plotted the H3K27ac signal against enhancer rank and used the tangent of the resulting curve to distinguish between SEs and typical enhancers (TEs) (Fig. 2a). Among 894 SEs defined in HIBEpiC cells. 355 super targeted genes showed particularly high expression levels, while 50 cancer-specific super targeted genes exhibited much lower expression in HIBEpiC cells (Fig. 2b).

HIBEpiC-SE-associated tumor suppressor genes *SMAD3*, *STAT1*, and *STAT4* showed much higher expression in the normal cell line and much lower expression in cancer cell lines (Fig. 2c). The H3K27ac signal in ICC is lower than normal cell line in *SMAD3*, *STAT1*, *STAT4*. Besides, there are large amounts of AP-1 motifs in *SMAD3*, *STAT1*, *STAT4* (Fig. 2d). Cancer cell line SE-associated genes exhibited low expression in the normal cell line and high expression in the cancer cell lines. These results demonstrate highly specific and robust establishment of ICC-SEs in ICC cells and a strong correlation between SE activity and associated gene expression, which suggests important roles of ICC SEs in ICC specific gene transcription. Motif scan analysis showed changed sites of H3K4me3, H3K4me1, and H3K27ac, which are enriched with “TCGAGTCA”. Using homer software, we predicted the transcription factor AP-1 family, which consists of proteins belonging to the *c-FOS*, *c-JUN*, *ATF*, and *JDP* families, is the most likely protein binding to this site [41]. Previous studies have reported that AP-1 is associated with histone H3 modification, and AP-1 has also been reported to play a key role in SE selection and chromatin accessibility [42]. Using the ENCODE database, we found almost half of the HIBEpiC-targeted SE genes are *c-JUN* /AP-1 targeted genes (Supplementary Fig. S2).

### 3.3. *c-JUN* plays a key role in cell death-related differentially expressed genes

Differentially expressed gene (DEG) analysis of the different cell lines was performed to identify changes in transcript levels in ICC (Fig. 3a). We annotated DEGs between the cancer cell lines and the normal cell line, and identified many cancer-related pathways including regulation of cell death and regulation of apoptosis (Fig. 3b). Among the DEGs, *c-JUN* demonstrated the greatest change and had obvious effects on ICC [2]. Fig. 3c shows a predicted cell death-related DEG interaction, generated using GeneMANIA software [43], that includes genomic, proteomic, and molecular network interactions from different online sources. We found *c-JUN* has the most nodes and edges, so *c-JUN* played a key role in ICC cell death (Supplementary Table S2). These results suggested changes between the ICC cell lines and the normal cell line are both cancer cell death-related and *c-JUN*-related. Additionally, we also found *c-JUN* expression had significant effects on patient survival based on prognosis analysis of ICC in TCGA datasets (Fig. 3d and Supplementary Fig. S3), as low expressions of *c-JUN* decreased the the median survival by more than half.



(caption on next page)

**Fig. 3.** c-JUN plays a key role in cell death and is associated with differentially expressed genes (DEGs) in ICC. a. Heatmaps representing the Z scores of gene expression levels (upper panel) across all cell lines. b. GO and KEGG analysis showing pathways associated with DEGs. c. DEGs involved in cell death (striped circles) and associations predicted by GeneMANIA. Each gene is represented by a node (circles). The node size is proportional to the degree of connectivity and the node colors represent the functions in which genes are involved. Lines represent the relationship between genes, and the line width is proportional to the confidence of the connection. d. Overall survival in ICC patients grouped by c-JUN expression level. e. Bar plot representing c-JUN expression level in these samples.

### 3.4. DEGs are associated with nucleosome occupancy profiles in ICC cell lines and the HIBEpic cell line

As previous studies have reported, MNase-seq signals variation shows up in different cell lines especially around transcription start sites (TSSs) for expressed (left) and silent (right) genes [44]. AP-1 plays an essential role in chromatin accessibility [42]. We profiled nucleosome occupancy of ICC cell lines by MNase-seq, which can determine precise nucleosome positioning. We performed nucleosome mapping in differentially expressed genes from RNA-Seq in ICC and control cell lines. There is a more stable nucleosome profile in ICC cell lines than the HIBEpic cell line of down-regulated ICC genes. Variable nucleosomes were enriched in up-regulated ICC-related genes (Fig. 4a, b). Especially in TSSs, different nucleosome profiles imply gene expression, which occurs through an effect of different binding sites of transcription factors.

Many cancer-related genes, including NRAS, MAPK8, and BRCA1, have different nucleosome occupancy profiles, suggesting that nucleosome profiles have essential roles in the development of ICC (Fig. 3c, d, Supplementary Fig. S4). Histone modification regulates nucleosome remodeling through Set1 as previously described [45]. Therefore, it is possible there is crosstalk between histone modification and nucleosome occupancy.

### 3.5. c-JUN influences cell death and plays a key role in ICC

AP-1 could regulate many key genes, including CCND2, ATF4, IL22RA22, MT1F, NFATC2, and NTRK2 [46]. Those target genes which includes a c-JUN binding site in close proximity to its TSS play a key role in ICC [47]. To investigate c-JUN binding site on the CCND2 promoter region in the ICC cell lines, signal enrichment of H3K27ac and c-JUN were detected by ChIP-qPCR. By analyzing the different peaks of ChIP-H3K27ac (Supplementary Table S3), we found that chr12:4378329–4378902 and chr12:4380202–434382936 were located in the CCND2 promoter region. According to the binding base site sequence of c-JUN, it is predicted that the CCND2 promoter region chr12: 4378329–4378902 and chr12: 4380202–434382936 may bind the sequence 5-ATGTCCTTATCCG-3 (Promoter 1), 5-TGTCTGAGGT-CACCCC-3 (Promoter 2), 5-CTTGCGTACCGC -3 (Promoter 3), 5-CTTGCGTACCGC -3 (Promoter 4). We designed the corresponding primers based on the above sequence, and randomly selected a sequence at the far end to design a pair of primers as a negative control (Supplementary Table S1). As shown in Fig. 5a, H3K27ac and c-JUN were enriched at the putative promoter regions of CCND2 in CCLP-1 and SSP-25 cell lines.

To determine whether c-JUN affects cell death and apoptosis in ICC, we overexpressed c-JUN genes in SSP-25 cell line and CCLP-1 cell line (Fig. 5b). Interestingly, after overexpression of c-JUN, significant apoptosis of intrahepatic cholangiocarcinoma tumor cells was observed (Fig. 5c). At the same time, knockdown of c-FOS inhibited apoptosis. There were significant phenotypic differences between empty vector-transfected and transgene-transfected cells (Supplementary Fig. S5).

### 3.6. AP-1 plays a key role in patient OS and PFS in ICC

We also examined the expression levels of c-JUN in cancer and paracancerous tissue using immunohistochemical staining. c-JUN was expressed in nucleoplasm and cytoplasm, which was consistent with previous reports. Our results indicated that c-JUN exhibited low

expression in cancer tissues (Fig. 6a). Moreover, we found that c-JUN, c-FOS, and CCND2 mRNA expression levels were significantly different between cancer and paracancerous tissues, and exhibit low expression in cancer tissues (Fig. 6b). 0.41 ICC patients were divided into high and low groups according to the median qPCR relative expression value of cancer tissues. Survival analysis found that low expression of c-JUN and c-FOS significantly affected patients' OS and PFS (Fig. 6c). The data demonstrate that AP-1 may play an essential role in the development of ICC.

## 4. Conclusion

Epigenetic disruption of progenitor cells is a common early event in many types of cancer, including colorectal cancer, glioma, and liver cancer [48]. Epigenetic changes also promote chromosomal instability in the development of cancer [49]. However, there is little knowledge of the role of epigenetic and transcript profiles in ICC. In this study, we analyzed histone modification profiles, transcript profiles, and MNase-seq in ICC cell lines. Our results suggest that AP-1 may play a key role in ICC. Previous studies have used the histone mark H3K4me1 to analyze gain and loss of enhancer activity in primary colon cancer lines relative to normal colon crypts and identified thousands of variant enhancer loci. Reproducible changes at enhancer elements have been shown to drive a specific transcriptional program to promote colon carcinogenesis [13]. It has also been reported that the histone mark H3K4me3 is associated with increased transcription elongation and enhancer activity of tumor-suppressor genes [50]. H3K27 acetylation is altered in many types of cancers [51,52].

SEs regulate cancer cell proliferation and cell identity as well as survival through the transcriptional regulation of genes that confer oncogenic traits and lineage specificity. Many SE-associated genes provide novel therapeutic targets for cancers [53]. Through H3K27ac analysis, we determined ICC-associated SEs. MNase-seq assays all nucleosomes comparing ATAC-seq are concentrated at regulatory nucleosomes [54]. As previous studies have reported, MNase-seq profiles is different in genome especially around TSSs between expressed and silent genes. For expressed genes, the nucleosome profiles are relatively dynamic. For silent genes, the nucleosome profiles are more stable [42]. Therefore, MNase-seq had an advantage over nucleosome profiles. Using MNase-seq, we found that the expression levels of many cancer-related genes are associated with the nucleosome profiles. Moreover, ChIP-qPCR experiments showed that c-JUN binding site on the CCND2 promoter region in the ICC cell lines. We found that c-JUN, c-FOS, and CCND2 mRNA expression levels are low expression in cancer tissue, compared to paracancerous tissue. Survival analysis found that low expression of c-JUN and c-FOS significantly affected patients' OS and PFS.

This study is the first report showing the global features of histone modification, transcript, and nucleosome profiles in ICC; we also show that the transcription factor AP-1 might be a key target gene in ICC by targeting oncogene such as CCND2.

Supplementary data to this article can be found online at <https://doi.org/10.1016/j.ygeno.2021.12.008>.

## Credit author statement

KH, YLF and SQA equally contributed to this study. KH, YLF, SQA and GAX were directly involved in the design and conduct of the study. KH, YLF, SQA and FL were involved in the collection, generation, management, analysis, and interpretation of the data. All authors were

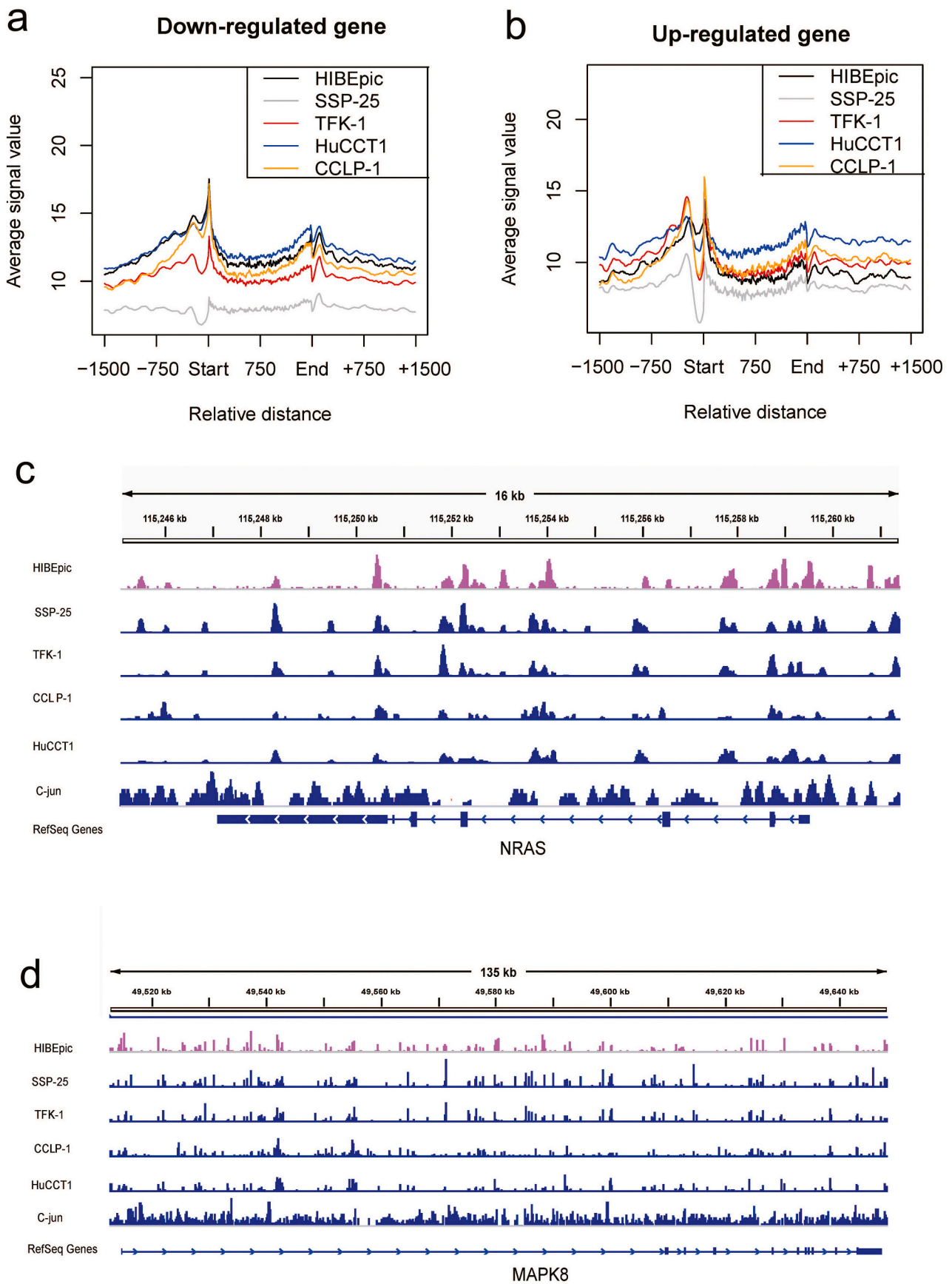


**Fig. 4.** Nucleosome occupancy profiling is associated with gene expression. a, b. Analysis of occupancy in the chromatin of downregulated and upregulated genes of ICC cell lines. c, d. MNase signals across the NRAS and MAPK8 loci associated with lost variant enhancer loci in these samples.

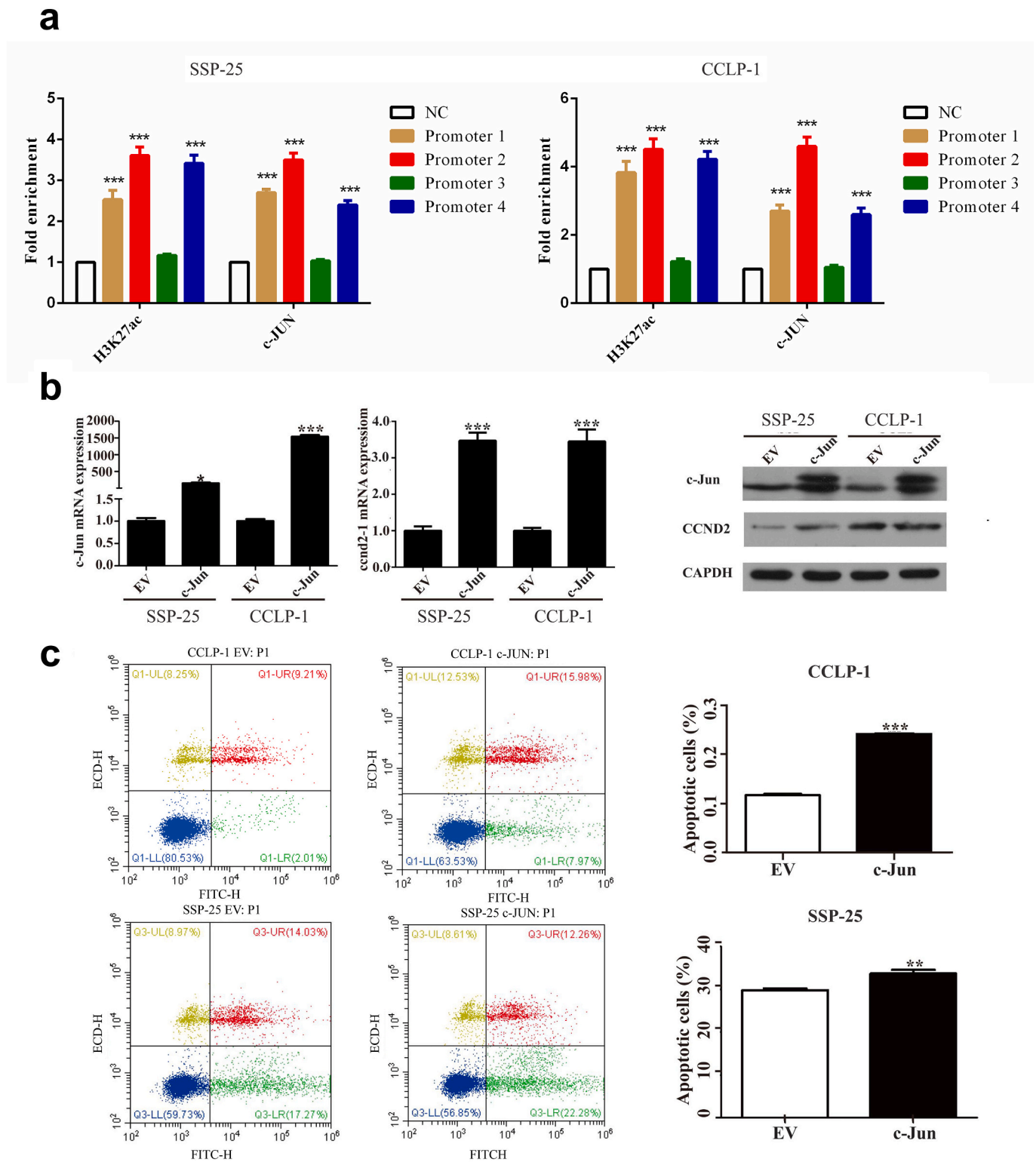


**Fig. 5.** AP1 influences cell death and plays a key role in ICC. **a.** H3K27ac and c-JUN enrichment in SSP-25 and CCLP-1 cells, as assessed by ChIP-qPCR and expressed as fold change over input normalized to the NC. **b.** Expression levels of CCND2 and c-JUN in SSP and CCLP cells after c-JUN overexpression. **c.** Flow cytometry analysis was used to detect apoptosis. Overexpression of c-JUN induced apoptosis in SSP-25 and CCLP-1 cells. Cells with c-JUN overexpression had greater rates of apoptosis compared with the cells transfected with empty vector.

involved in the preparation, review, and approval of the manuscript, and decision to submit the manuscript for publication.

**Funding**

This work was supported by grant from the National Natural Science Foundation of China (No. 81071990, No. 81641110) and 3D Printing

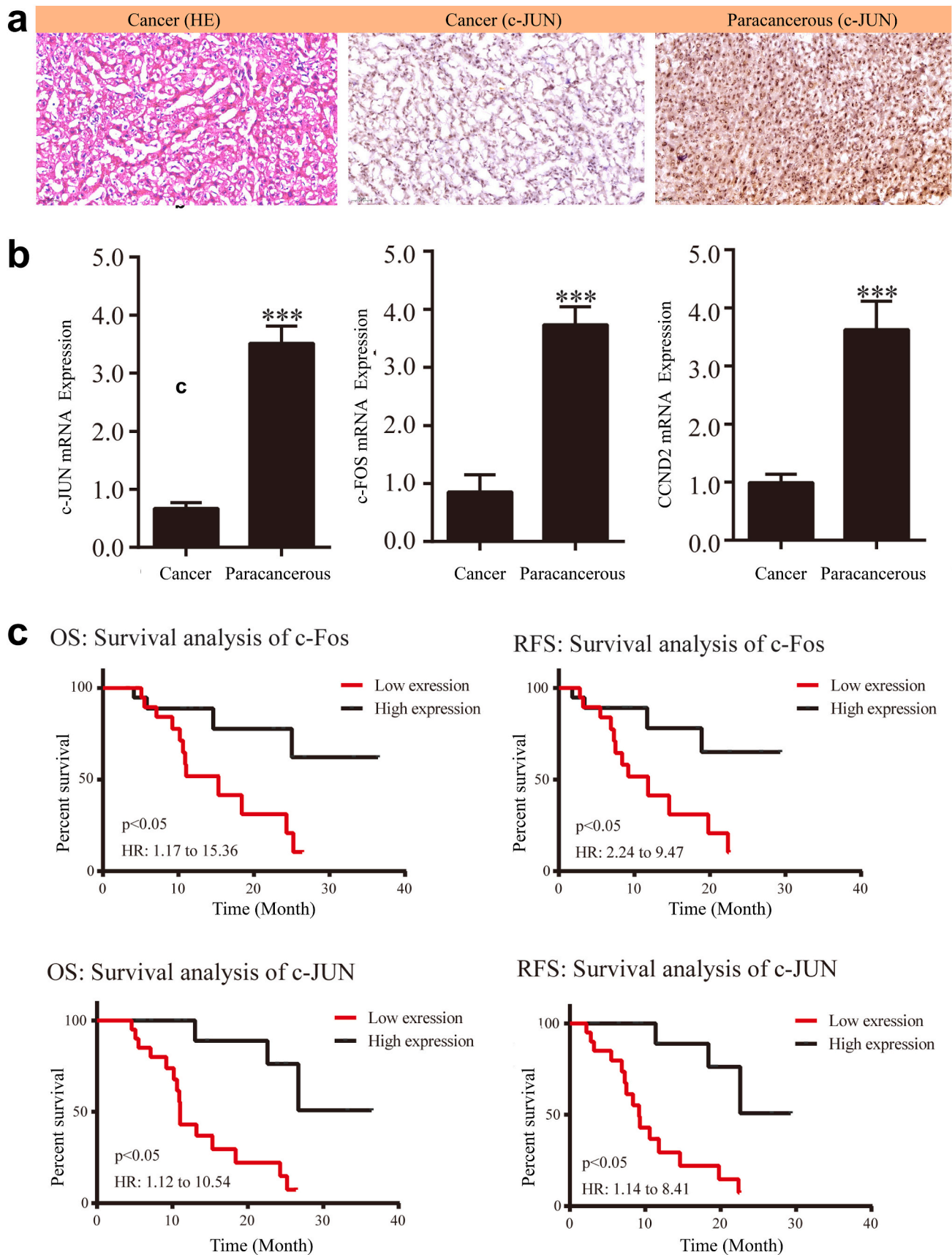


**Fig. 6.** AP-1 plays a key role in patients' OS and PFS in ICC. a. Representative images of staining of c-JUN protein in a pair of ICC patient's cancer and paracancerous tissue (20×). b. c-JUN, c-FOS, and CCND2 mRNA expression levels are significantly different between cancer and paracancerous tissues, and have low expression in cancer tissue. c. Survival analysis found that low expression of c-JUN and c-FOS significantly affected patients' OS and PFS.

Research Project (2020) of Guangdong Second Provincial General Hospital (No. 3D-A2020001).

## References

- [1] E.W. Beal, D. Tumin, D. Moris, X. Zhang, J. Chakedis, M. Dilhoff, C.M. Schmidt, T. M. Pawlik, Cohort contributions to trends in the incidence and mortality of intrahepatic cholangiocarcinoma, *Hepatob. Surg. Nutr.* 7 (2018) 270.
- [2] X. Chen, Y. Yin, J. Cheng, A. Huang, B. Hu, X. Zhang, Y. Sun, J. Wang, Y. Wang, Y. Ji, BAP1 acts as a tumor suppressor in intrahepatic cholangiocarcinoma by modulating the ERK1/2 and JNK/c-JUN pathways, *Cell Death Dis.* 9 (2018) 1–14.
- [3] L. Liu, Z. Lang, P. Wang, H. Wang, Y. Cao, X. Meng, J. Hu, Y. Feng, The nucleosome binding protein 1 promotes the growth of gastric cancer cells, *J. Cancer* 10 (2019) 1132.
- [4] C. Lu, D. Yang, M.E. Sabbatini, A.H. Colby, M.W. Grinstaff, N.H. Oberlies, C. Pearce, K. Liu, Contrasting roles of H3K4me3 and H3K9me3 in regulation of apoptosis and gemcitabine resistance in human pancreatic cancer cells, *BMC Cancer* 18 (2018) 149.
- [5] H. Liu, Y. Li, J. Li, Y. Liu, B. Cui, H3K4me3 and Wdr82 are associated with tumor progression and a favorable prognosis in human colorectal cancer, *Oncol. Lett.* 16 (2018) 2125–2134.
- [6] K. Wang, S. Shan, S. Wang, X. Gu, X. Zhou, T. Ren, HMGB1-containing nucleosome mediates chemotherapy-induced metastasis of human lung cancer, *Biochem. Biophys. Res. Commun.* 500 (2018) 758–764.
- [7] J. Högstöm, S. Heino, P. Kallio, M. Lähde, V. Leppänen, D. Balboa, Z. Wiener, K. Alitalo, Transcription factor PROX1 suppresses Notch pathway activation via the nucleosome remodeling and deacetylase complex in colorectal cancer stem-like cells, *Cancer Res.* 78 (2018) 5820–5832.
- [8] K. Triff, M.W. McLean, K. Konganti, J. Pang, E. Callaway, B. Zhou, I. Ivanov, R. S. Chapkin, Assessment of histone tail modifications and transcriptional profiling during colon cancer progression reveals a global decrease in H3K4me3 activity, *Biochim. Biophys. Acta* 1863 (2017) 1392–1402.
- [9] P. McAnena, J.A. Brown, M.J. Kerin, Circulating nucleosomes and nucleosome modifications as biomarkers in cancer, *Cancers* 9 (2017) 5.
- [10] R. Watanabe, S. Kanno, A. Mohammadi Roushandeh, A. Ui, A. Yasui, Nucleosome remodelling, DNA repair and transcriptional regulation build negative feedback loops in cancer and cellular ageing, *Philos. Trans. R. Soc. B* 372 (2017) 20160473.
- [11] C. Lu, A.V. Paschall, H. Shi, N. Savage, J.L. Waller, M.E. Sabbatini, N.H. Oberlies, C. Pearce, K. Liu, The MLL1-H3K4me3 axis-mediated PD-L1 expression and pancreatic cancer immune evasion, *JNCI* 109 (2017).
- [12] J.M. Spangle, K.M. Dreijerink, A.C. Groner, H. Cheng, C.E. Ohlson, J. Reyes, C. Y. Lin, J. Bradner, J.J. Zhao, T.M. Roberts, PI3K/AKT signaling regulates H3K4 methylation in breast cancer, *Cell Rep.* 15 (2016) 2692–2704.
- [13] B. Akhtar-Zaidi, R. Cowper-Sal, O. Corradin, A. Saiakhova, C.F. Bartels, D. Balasubramanian, L. Myeroff, J. Lutterbaugh, A. Jarrar, M.F. Kalady, Epigenomic enhancer profiling defines a signature of colon cancer, *Science* 336 (2012) 736–739.
- [14] A. Kremer, S. Holdenrieder, P. Stieber, R. Wilkowski, D. Nagel, D. Seidel, Nucleosomes in colorectal cancer patients during radiochemotherapy, *Tumor Biol.* 27 (2006) 235–242.
- [15] C. Iannone, A. Pohl, P. Papisaikas, D. Soronellas, G.P. Vicent, M. Beato, J. Valcárcel, Relationship between nucleosome positioning and progesterone-induced alternative splicing in breast cancer cells, *RNA* 21 (2015) 360–374.
- [16] T. Nakaoka, Y. Saito, H. Saito, Aberrant DNA methylation as a biomarker and a therapeutic target of cholangiocarcinoma, *Int. J. Mol. Sci.* 18 (2017).
- [17] C.J. O'Rourke, P. Munoz-Garrido, E.L. Aguayo, J.B. Andersen, Epigenome dysregulation in cholangiocarcinoma, *Biochim. Biophys. Acta Mol. basis Dis.* 1864 (2018) 1423–1434.
- [18] Q. Zhao, R. Wirka, T. Nguyen, M. Nagao, P. Cheng, C.L. Miller, J.B. Kim, M. Pjanic, T. Quettermous, TCF21 and AP-1 interact through epigenetic modifications to regulate coronary artery disease gene expression, *Genome Med.* 11 (2019) 23.
- [19] H. He, I. Sinha, R. Fan, L. Haldosen, F. Yan, C. Zhao, K. Dahlman-Wright, c-JUN/AP-1 overexpression reprograms ER $\alpha$  signaling related to tamoxifen response in ER $\alpha$ -positive breast cancer, *Oncogene* 37 (2018) 2586–2600.
- [20] S. Wolter, A. Doerrie, A. Weber, H. Schneider, E. Hoffmann, J. von der Ohe, L. Bakiri, E.F. Wagner, K. Resch, M. Kracht, c-JUN controls histone modifications, NF- $\kappa$ B recruitment, and RNA polymerase II function to activate the ccl2 gene, *Mol. Cell. Biol.* 28 (2008) 4407–4423.
- [21] Y. Abuetabh, S. Persad, S. Nagamori, J. Huggins, R. Al-Bahrani, C. Sergi, Expression of E-cadherin and  $\beta$ -catenin in two cholangiocarcinoma cell lines (OZ and HuCCT1) with different degree of invasiveness of the primary tumor, *Ann. Clin. Lab. Sci.* 41 (2011) 217–223.
- [22] S. Baek, Y. Lee, S. Yoon, S. Baek, B. Kim, S. Oh, CDH3/P-Cadherin regulates migration of HuCCT1 cholangiocarcinoma cells, *Anatomy Cell Biol.* 43 (2010) 110–117.
- [23] J. Iwaki, K. Kikuchi, Y. Mizuguchi, Y. Kawahigashi, H. Yoshida, E. Uchida, T. Takizawa, MiR-376c down-regulation accelerates EGF-dependent migration by targeting GRB2 in the HuCCT1 human intrahepatic cholangiocarcinoma cell line, *PLoS One* 8 (2013).
- [24] T. Shimada, T. Imaizumi, K. Shirai, T. Tatsuta, T. Kimura, R. Hayakari, H. Yoshida, T. Matsumiya, H. Kijima, H. Mizukami, CCL5 is induced by TLR 3 signaling in HuCCT1 human biliary epithelial cells: possible involvement in the pathogenesis of biliary atresia, *Biomed. Res.* 38 (2017) 269–276.
- [25] Y. Xu, J. Cui, L. Zhang, D. Zhang, B. Xing, X. Huang, J. Wu, C. Liang, G. Li, Anti-apoptosis effect of Decoy receptor 3 in cholangiocarcinoma cell line TFK-1, *Chin. Med. J.* 131 (2018) 82.
- [26] H.H. He, C.A. Meyer, M.W. Chen, V.C. Jordan, M. Brown, X.S. Liu, Differential DNase I hypersensitivity reveals factor-dependent chromatin dynamics, *Genome Res.* 22 (2012) 1015–1025.
- [27] D. Kim, B. Langmead, S.L. Salzberg, HISAT: a fast spliced aligner with low memory requirements, *Nat. Methods* 12 (2015) 357–360.
- [28] M. Pertea, D. Kim, G.M. Pertea, J.T. Leek, S.L. Salzberg, Transcript-level expression analysis of RNA-seq experiments with HISAT, StringTie and Ballgown, *Nat. Protoc.* 11 (2016) 1650.
- [29] I. Lindner, D. Rubin, U. Helwig, I. Nitz, J. Hampe, S. Schreiber, J. Schrezenmeir, F. Döring, The L513S polymorphism in medium-chain acyl-CoA synthetase 2 (MACS2) is associated with risk factors of the metabolic syndrome in a Caucasian study population, *Mol. Nutr. Food Res.* 50 (2006) 270–274.
- [30] K. Chen, Y. Xi, X. Pan, Z. Li, K. Kaestner, J. Tyler, S. Dent, X. He, W. Li, DANPOS: dynamic analysis of nucleosome position and occupancy by sequencing, *Genome Res.* 23 (2013) 341–351.
- [31] W.B. Langdon, Performance of genetic programming optimised Bowtie2 on genome comparison and analytic testing (GCAT) benchmarks, *BioData Min.* 8 (2015) 1.
- [32] R.C. Gentleman, V.J. Carey, D.M. Bates, B. Bolstad, M. Dettling, S. Dudoit, B. Ellis, L. Gautier, Y. Ge, J. Gentry, Bioconductor: open software development for computational biology and bioinformatics, *Genome Biol.* 5 (2004) R80.
- [33] H. Thorvaldsdóttir, J.T. Robinson, J.P. Mesirov, Integrative Genomics Viewer (IGV): high-performance genomics data visualization and exploration, *Brief. Bioinform.* 14 (2013) 178–192.
- [34] B.T. Sherman, R.A. Lempicki, Systematic and integrative analysis of large gene lists using DAVID bioinformatics resources, *Nat. Protoc.* 4 (2009) 44.
- [35] C.L. Callahan, M.R. Bonner, J. Nie, Y. Wang, M. Tao, P.G. Shields, C. Marian, K. H. Eng, M. Trevisan, J.L. Freudenheim, Active and secondhand smoke exposure throughout life and DNA methylation in breast tumors, *Cancer Causes Control* 30 (2019) 53–62.
- [36] M. Hua, Y. Qin, M. Sheng, X. Cui, W. Chen, J. Zhong, J. Yan, Y. Chen, miR-145 suppresses ovarian cancer progression via modulation of cell growth and invasion by targeting CCND2 and E2F3, *Mol. Med. Rep.* 19 (2019) 3575–3583.
- [37] L. Yang, F. Ye, L. Bao, X. Zhou, Z. Wang, P. Hu, N. Ouyang, X. Li, Y. Shi, G. Chen, Somatic alterations of TP53, ERBB2, PIK3CA and CCND1 are associated with chemosensitivity for breast cancers, *Cancer Sci.* 110 (2019) 1389.
- [38] Y. Deng, S. Luo, C. Deng, T. Luo, W. Yin, H. Zhang, Y. Zhang, X. Zhang, Y. Lan, Y. Ping, Y. Xiao, X. Li, Identifying mutual exclusivity across cancer genomes: computational approaches to discover genetic interaction and reveal tumor vulnerability, *Brief. Bioinform.* 20 (2017) 254–266.
- [39] L. Chang, R. Guo, Z. Yuan, H. Shi, D. Zhang, LncRNA HOTAIR regulates CCND1 and CCND2 expression by sponging miR-206 in ovarian cancer, *Cell. Physiol. Biochem.* 49 (2018) 1289–1303.
- [40] W.A. Whyte, D.A. Orlando, D. Hnisz, B.J. Abraham, C.Y. Lin, M.H. Kagey, P. B. Rahl, T.I. Lee, R.A. Young, Master transcription factors and mediator establish super-enhancers at key cell identity genes, *Cell* 153 (2013) 307–319.
- [41] S. Heinz, C. Benner, N. Spann, E. Bertolino, Y.C. Lin, P. Laslo, J.X. Cheng, C. Murre, H. Singh, C.K. Glass, Simple combinations of lineage-determining transcription factors prime cis-regulatory elements required for macrophage and B cell identities, *Mol. Cell* 38 (2010) 576–589.
- [42] P. Madrigal, K. Alasoo, AP-1 takes centre stage in enhancer chromatin dynamics, *Trends Cell Biol.* 28 (2018) 509–511.
- [43] J. Montojo, K. Zuberi, H. Rodriguez, G.D. Bader, Q. Morris, GeneMANIA: Fast gene network construction and function prediction for Cytoscape, *F1000Research* 3 (2014).
- [44] J. Mieczkowski, A. Cook, S.K. Bowman, B. Mueller, B.H. Alver, S. Kundu, A. M. Deaton, J.A. Urban, E. Larschan, P.J. Park, MNase titration reveals differences between nucleosome occupancy and chromatin accessibility, *Nat. Commun.* 7 (2016) 11485.
- [45] S. Wang, B.O. Zhou, J. Zhou, Histone H3 lysine 4 hypermethylation prevents aberrant nucleosome remodeling at the PHO5 promoter, *Mol. Cell. Biol.* 31 (2011) 3171–3181.
- [46] C. Zhao, Y. Qiao, P. Jonsson, J. Wang, L. Xu, P. Rouhi, I. Sinha, Y. Cao, C. Williams, K. Dahlman-Wright, Genome-wide profiling of AP-1-regulated transcription provides insights into the invasiveness of triple-negative breast cancer, *Cancer Res.* 74 (2014) 3983–3994.
- [47] N. Martinez-Soria, L. McKenzie, J. Draper, A. Ptasinska, H. Issa, S. Potluri, H. J. Blair, A. Pickin, A. Isa, P.S. Chin, The oncogenic transcription factor RUNX1/ETO corrupts cell cycle regulation to drive leukemic transformation, *Cancer Cell* 34 (2018) 626–642, e8.
- [48] W. Ma, C. Han, J. Zhang, K. Song, W. Chen, H. Kwon, T. Wu, The histone methyltransferase G9a promotes cholangiocarcinogenesis through regulation of the Hippo pathway kinase LATS2 and YAP signaling pathway, *Hepatology.* 72 (4) (2021) 1283–1297.
- [49] A.P. Feinberg, R. Ohlsson, S. Henikoff, The epigenetic progenitor origin of human cancer, *Nat. Rev. Genet.* 7 (2006) 21–33.
- [50] K. Chen, Z. Chen, D. Wu, L. Zhang, X. Lin, J. Su, B. Rodriguez, Y. Xi, Z. Xia, X. Chen, Broad H3K4me3 is associated with increased transcription elongation and enhancer activity at tumor-suppressor genes, *Nat. Genet.* 47 (2015) 1149.
- [51] M.P. Creighton, A.W. Cheng, G.G. Weistead, T. Kooistra, B.W. Carey, E.J. Steine, J. Hanna, M.A. Lodato, G.M. Frampton, P.A. Sharp, Histone H3K27ac separates active from poised enhancers and predicts developmental state, *Proc. Natl. Acad. Sci.* 107 (2010) 21931–21936.

- [52] Q. Li, D. Wang, L. Ju, J. Yao, C. Gao, P. Lei, L. Li, X. Zhao, M. Wu, The hyper-activation of transcriptional enhancers in breast cancer, *Clin. Epigenetics* 11 (2019) 48.
- [53] T. Sanda, R.W. Wong, P.T. Cao, W.Z. Leong, A.W. Yam, T. Zhang, S. Iida, T. Okamoto, R. Ueda, N.S. Gray, Identification of Super-Enhancer-Associated Cancer Genes Provides Novel Therapeutic Targets in Adult T-cell Leukemia/Lymphoma, *AACR*, 2017.
- [54] J.D. Buenrostro, P.G. Giresi, L.C. Zaba, H.Y. Chang, W.J. Greenleaf, Transposition of native chromatin for fast and sensitive epigenomic profiling of open chromatin, DNA-binding proteins and nucleosome position, *Nat. Methods* 10 (2013) 1213.